MT25

25th International Conference on Magnet Technology

LANZHOU UNIVERSITY

Analytical investigation in bending characteristic of pre-twisted HTS tapes

Wurui Ta, Yuanwen Gao

Department of Mechanics and Engineering Sciences, College of Civil Engineering and Mechanics, Lanzhou University, Lanzhou, Gansu 730000, P.R. China

Email：tawr@lzu.edu.cn

Aug 27-Sep 1, 2017, Amsterdam, Netherlands

Contents

- Introduction
- Model description
- Results
- Conclusions

Contents

LANZHOU UNIVERSITY

The application of superconductor：ITER Tokamak

- The Tokamak magnet system consists of six poloidal field (**PF**) coils, 18 longitudinal toroidal (**TF**) coils, a central solenoid (**CS**) coil, and 18 correction Coils (**CC**) coils.
- The coils are all made of cable in conduit conductor (CICC).
- CICC is made of low temperature superconducting strands (Nb_3Sn / NbTi) through multi-level twist.

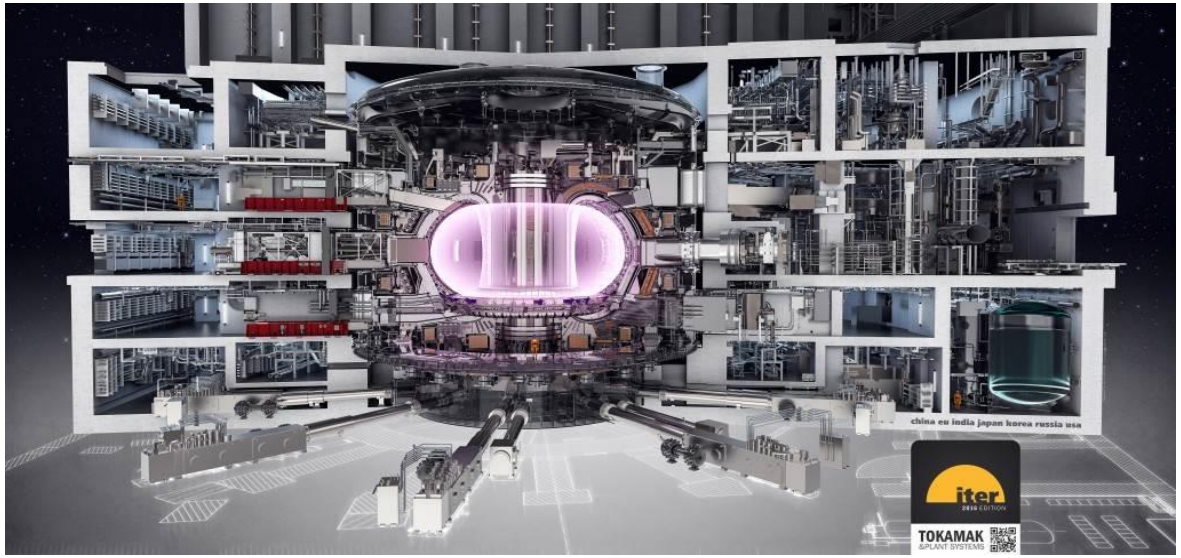

ITER Tokamak

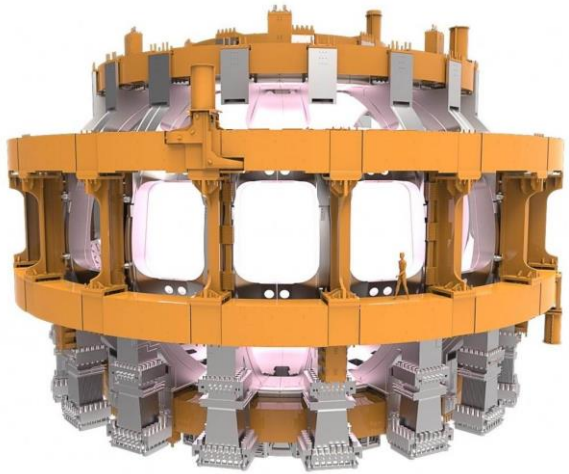

PF Coils

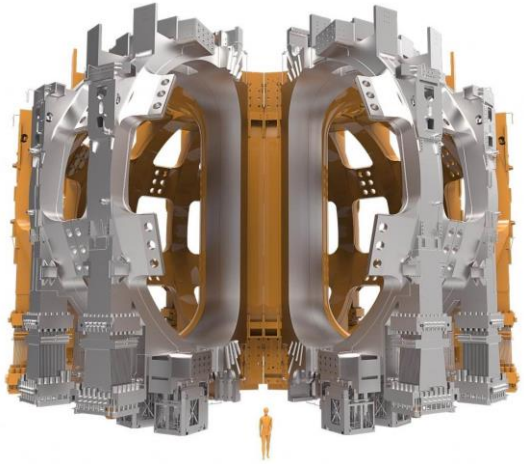

TF Coils

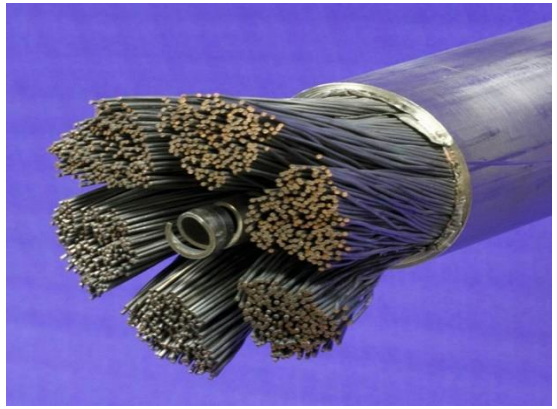

CICC

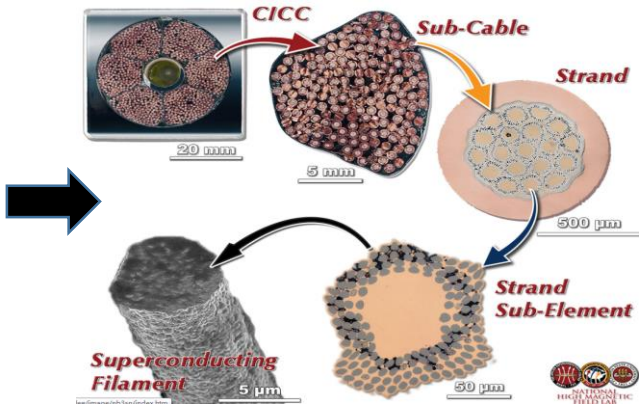

http://www.iter.org

LANZHOU UNIVERSITY

HTS fusion cable concept

- The second generation high temperature superconductors (2G HTS) exhibit high critical magnetic fields, high current densities, specific heats, thermal conductivities, and low required refrigeration power.

- Several HTS cable structures suitable for fusion reactor magnets are proposed, such as the helical twisted stacking-tape cable (TSTC), the twisted-stack slotted-core (TSSC) HTS cable and the conductor on round core (CORC) cable.

- The superconducting tapes are stacked and twisted inside the cable.

- The cable is subjected to transverse Lorentz force when it is run, and its transport performance is mainly determined by the **pre-twisted** superconducting tape.

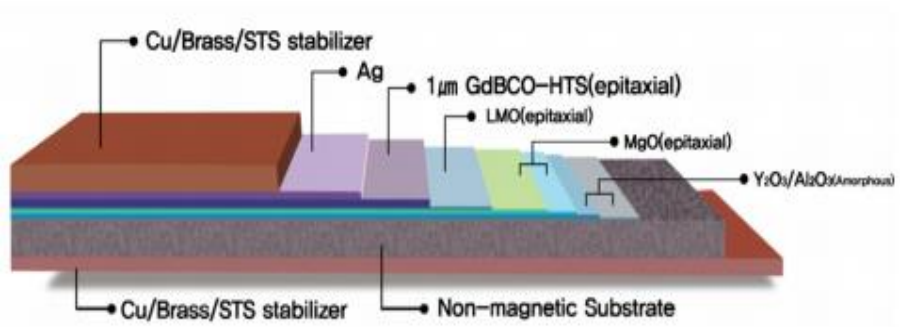

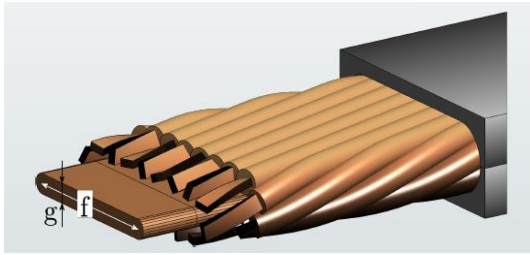

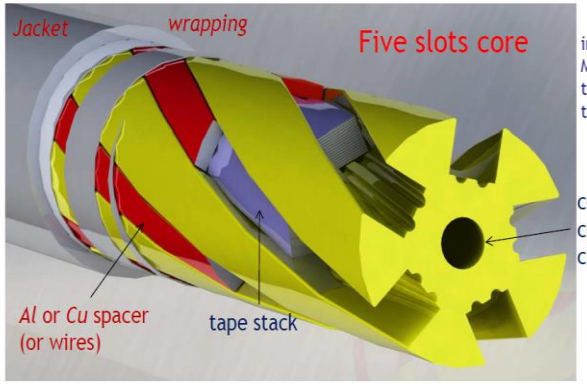

inspired by the MIT concept for twisted-stacked tape CICC

cooling central channel

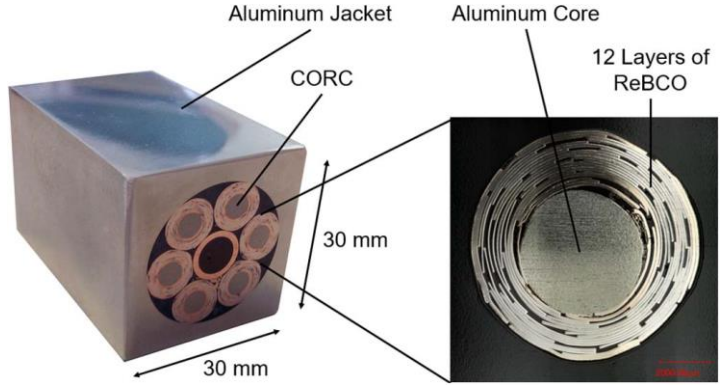

1. *Mulder T et al,IEEE Transactions on Applied Superconductivity, 2016, 26(3): 1-4.*
2. *Takayasu M et al., IEEE Transactions on Applied Superconductivity, 2016, 26(2): 25-34.*
3. *Celentano G et al., IEEE transactions on applied superconductivity, 2014, 24(3): 1-5.*

LANZHOU UNIVERSITY

Motivation

- How to improve the mechanical properties of the pre-twisted HTS tape against the transverse Lorentz force ?

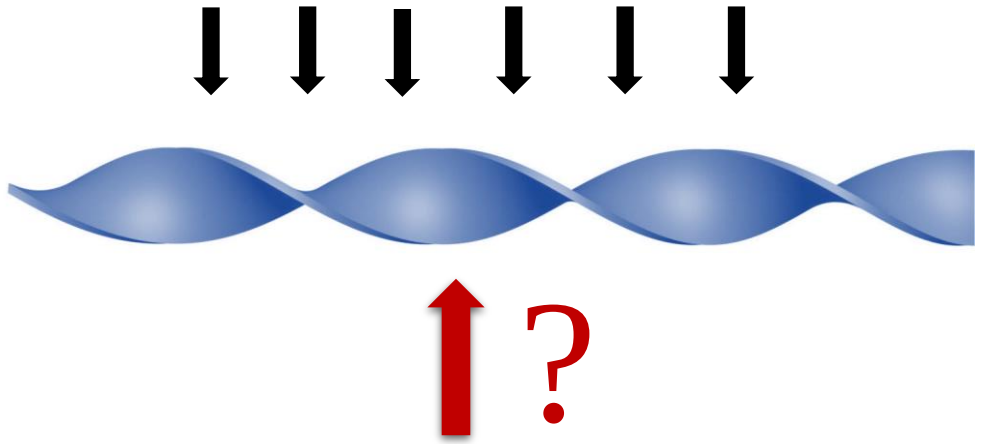

- How the twisting morphology affects the electromagnetic characteristics of HTS tape.

LANZHOU UNIVERSITY

Previous work

- A longitudinal strain model taking into account the internal shortening compressive strains accompanied with the tensile longitudinal strains due to a torsional twist was proposed by Takayasu M. The critical current of a twisted tape is given by the integration of the critical current densities corresponding to the strain distribution over the tape cross-section. *Takayasu M et al., AIP Conference Proceedings. AIP, 2010, 1219(1): 337-344.*

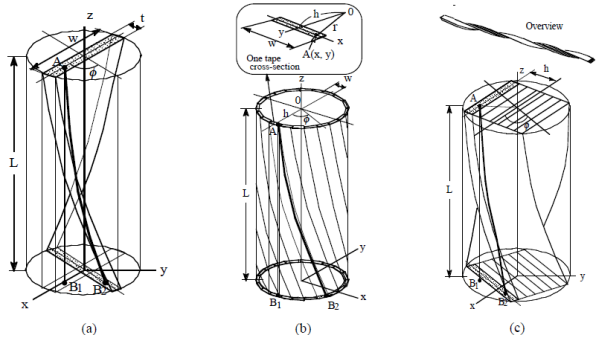

$$\varepsilon_x = \frac{1}{2}\left(\frac{\gamma_{\max}}{t}\right)^2\left(x^2 - \frac{w^2}{12}\right)$$

$$\varepsilon_{\max} = \frac{w^2\theta^2}{12} = \frac{w^2}{12}\left(\frac{\gamma_{\max}}{t}\right)^2$$

$$\varepsilon_{\min} = -\frac{w^2\theta^2}{24} = -\frac{w^2}{24}\left(\frac{\gamma_{\max}}{t}\right)^2$$

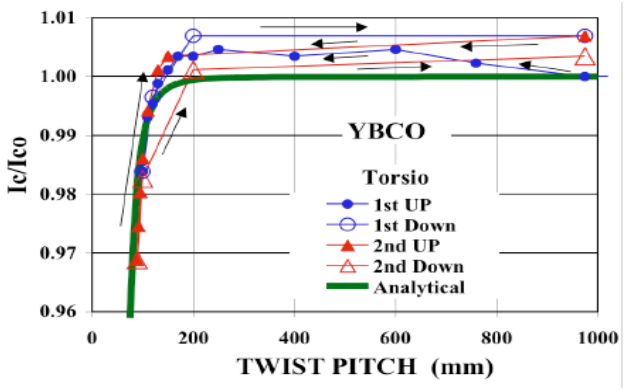

- A generalized empirical degradation model based on Ekin's exponential model and Weibull's distribution function is developed for capturing the critical current degradation behavior under different deformation modes. *Gao P et al. IEEE Transactions on Applied Superconductivity, 2016, 26(4): 1-5.*

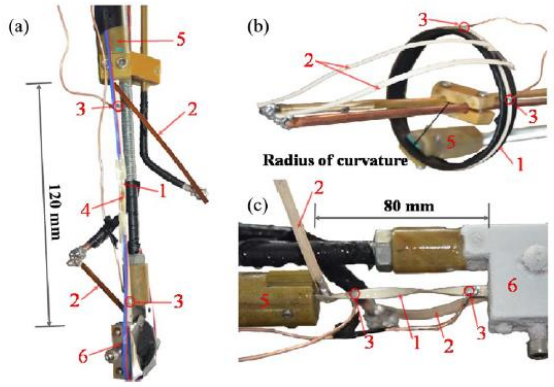

$$\frac{I_T}{I_0} = \begin{cases} 1 - a|\varepsilon|^2 & \varepsilon \le \varepsilon_{\mathrm{irr}} \\ (1 - a|\varepsilon|^2)\exp\left[-\left(\frac{\varepsilon - \varepsilon_{\mathrm{irr}}}{\varepsilon_0}\right)^2\right] & \varepsilon > \varepsilon_{\mathrm{irr}} \end{cases}$$

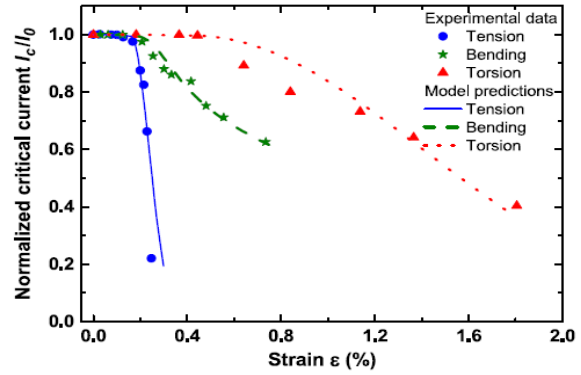

LANZHOU UNIVERSITY

Previous work

- The I_c degradation behaviors including the reversible variation of I_c have been investigated in YBCO coated conductor under torsional deformation. *Shin H S et al.IEEE Transactions on Applied Superconductivity, 2007, 17(2): 3274-3277.*

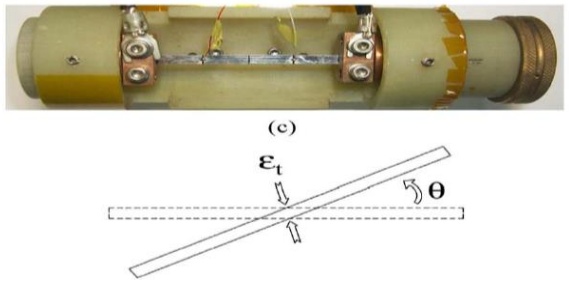

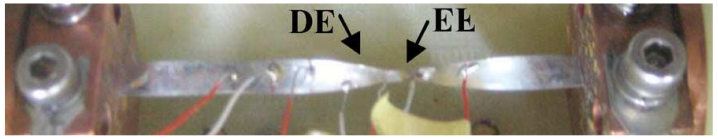

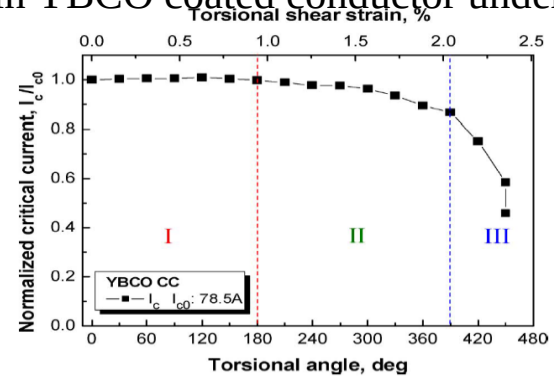

- Effects of transverse loads on single tapes and TSTC conductors were studied to evaluate and compare their mechanical behaviors.

Chiesa L et al. IEEE Transactions on Applied Superconductivity, 2014, 24(3): 1-5.

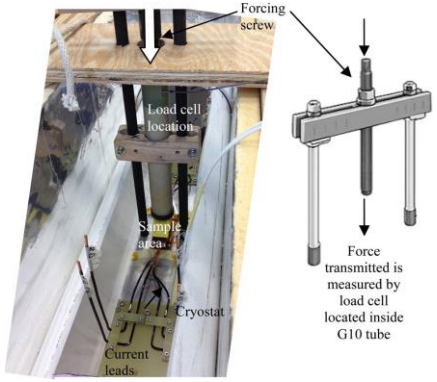

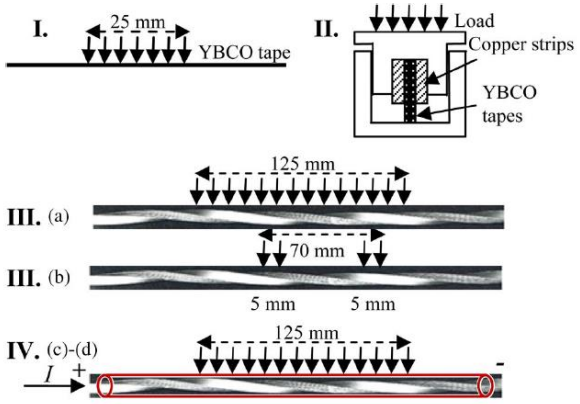

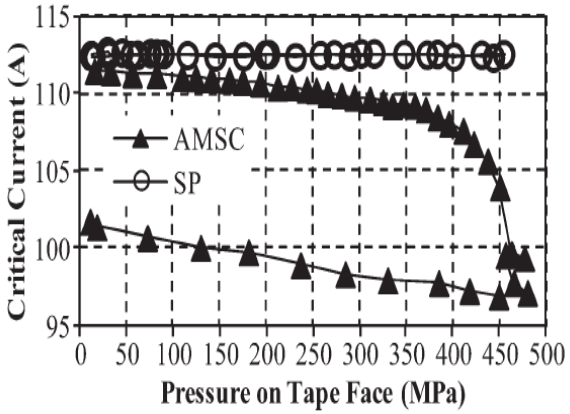

➢ The focus of these works is the effect of strain on critical current under twist load. However, there are few theoretical models on the pre-twisted tape subjected to transverse Lorentz force.

Contents

LANZHOU UNIVERSITY

Mechanical model

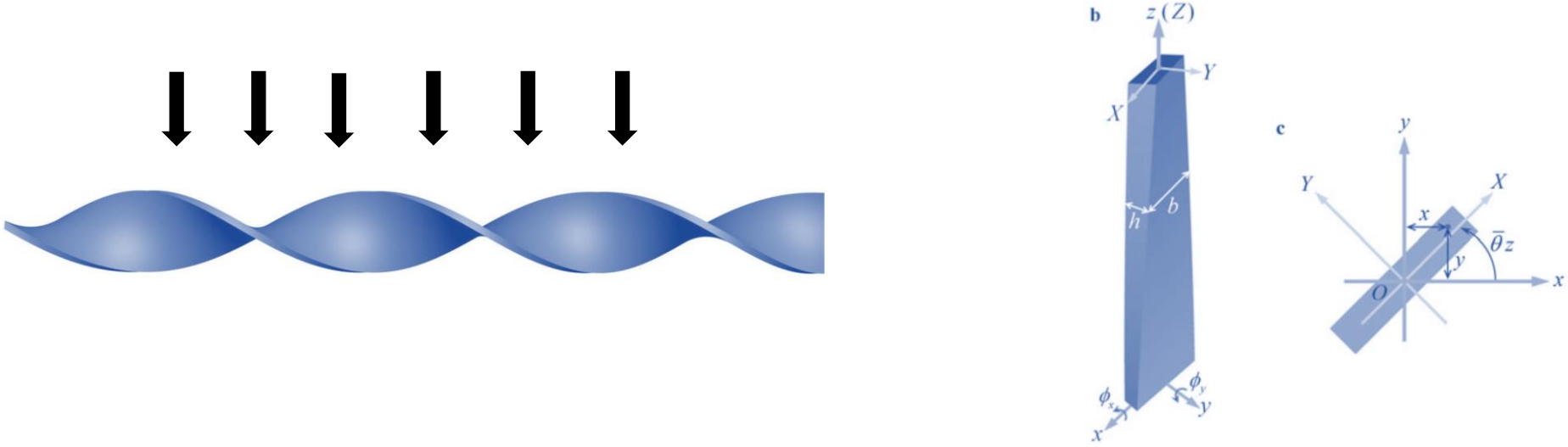

A pre-twisted rectangular beam; Its model with the global coordinate system (x, y, z) and local coordinate system(X, Y, Z), and **c** the rectangular cross section

In terminology of the Timoshenko beam theory, introduce four generalized displacements: u_x and u_y denote the deflections of the cross-sectional centroid, φ_x and φ_y denote the rotating angles of its cross section in the x and y directions, respectively. The cross section has the pre-existed rotating angle θz about the z axis. The normal strain at position (x, y, z) is written as

$$\varepsilon_z = x\frac{d\phi_y}{dz} + y\frac{d\phi_x}{dz}$$

Mechanical model

Assume that the material is linear elastic and isotropic. Then the bending moments M_x and M_y along the x and y directions on the cross section can be derived as

$$M_x = \iint_A E\varepsilon_z y dA = EI_{xx}\frac{d\phi_x}{dz} + EI_{xy}\frac{d\phi_y}{dz}$$

$$M_y = \iint_A E\varepsilon_z x dA = EI_{xy}\frac{d\phi_x}{dz} + EI_{yy}\frac{d\phi_y}{dz}$$

where E is the Young's modulus and A represents the cross sectional area of the beam.

The area moments of inertia I_{xx} and I_{yy}, and the polar moment of area I_{xy} are expressed as

$$I_{xx} = I_X \cos^2(\bar{\theta}z) + I_Y \sin^2(\bar{\theta}z)$$

$$I_{yy} = I_X \sin^2(\bar{\theta}z) + I_Y \cos^2(\bar{\theta}z)$$

$$I_{xy} = (I_Y - I_X)\sin(\bar{\theta}z)\cos(\bar{\theta}z)$$

where $I_X = bh^3/12$ and $I_Y = b^3h/12$ designate the principal area moments of inertia of the cross section.

Mechanical model

We analyze the pre-twisted beam by using the principle of minimum potential energy. The elastic strain energy of the beam due to bending can be calculated by

$$U_{\mathrm{b}} = \frac{1}{2}\int_0^L \left[EI_{xx}\left(\frac{d\phi_x}{dz}\right)^2 + 2EI_{xy}\frac{d\phi_x}{dz}\frac{d\phi_y}{dz} + EI_{yy}\left(\frac{d\phi_y}{dz}\right)^2 \right] dz$$

Besides, the elastic strain energy U_{s} of the beam due to shear deformation is

$$U_{\mathrm{s}} = \frac{1}{2}\int_0^L \kappa GA\left[\left(\frac{du_x}{dz} - \phi_y\right)^2 + \left(\frac{du_y}{dz} - \phi_x\right)^2 \right] dz$$

where $G = E/[2(1 + \nu)]$ is the shear modulus and κ is the shearing correction factor. For rectangular beams, κ is ascertained as 0.83. Consequently, the total elastic strain energy U of the beam is

$$U = U_b + U_s$$

Mechanical model

we here investigate the bending property of the pre-twisted beam subjected to periodically distributed transverse force. Then the transverse force f_y with intensity $\bar{f}_y$ perunit area has the form of

$$f_y = f_1 + f_2\left|\cos\left(\bar{\theta}z\right)\right|$$

where $f_1 = h\bar{f}_y$ and $f_2 = (b-h)\bar{f}_y$.

The potential energy V_f of the external forces is written as

$$V_f = -\int_0^L \left[f_1 + f_2\cos\left(\bar{\theta}z\right)\right]u_y dz$$

Let $\Pi = U + V_f$ denote the total potential energy of the beam system. According to the principle of minimum potential energy, the beam at the equilibrium state has the following vibrational relation

$$\delta\prod = \delta\left(U + V_f\right) = 0$$

Note that due to the chiral morphology of the beam, the force in the y direction will induce both deflections in the x and y directions, u_x and u_y.

LANZHOU UNIVERSITY

Mechanical model

A set of static equilibrium equations and eight boundary conditions of the pre-twisted beam are obtained

$$\begin{cases} \dfrac{d^2u_x}{dz^2}=\dfrac{d\phi_y}{dz} & ① \\ \dfrac{d^2u_y}{dz^2}=-\dfrac{f_1+f_2\cos(\bar{\theta}z)}{\kappa GA}+\dfrac{d\phi_x}{dz} & ② \\ \dfrac{d}{dz}\left(I_{xx}\dfrac{d\phi_x}{dz}+I_{xy}\dfrac{d\phi_y}{dz}\right)=\dfrac{\kappa GA}{E}\left(\phi_x-\dfrac{du_y}{dz}\right) & ③ \\ \dfrac{d}{dz}\left(I_{xy}\dfrac{d\phi_x}{dz}+I_{yy}\dfrac{d\phi_y}{dz}\right)=\dfrac{\kappa GA}{E}\left(\phi_y-\dfrac{du_x}{dz}\right) & ④ \end{cases}$$

$$u_x\big|_{z=0}=u_y\big|_{z=0}=\phi_x\big|_{z=0}=\phi_y\big|_{z=0}=0$$

$$u_x\big|_{z=L}=u_y\big|_{z=L}=\left(EI_{xx}\frac{d\phi_x}{dz}+EI_{xy}\frac{d\phi_y}{dz}\right)\Bigg|_{z=L}=\left(EI_{yy}\frac{d\phi_y}{dz}+EI_{xy}\frac{d\phi_x}{dz}\right)\Bigg|_{z=L}=0$$

LANZHOU UNIVERSITY

Mechanical model

Finally, the deflections in the *x* and *y* directions are derived as

$$
\begin{aligned}
u_x = {} & \frac{(1-\mu^2)f_1}{16I_Y E\bar{\theta}^4}\left(-\alpha^2\sin(2\alpha)-2\alpha\cos(2\alpha)-\alpha+\frac{3}{2}\sin(2\alpha)+\theta^2\sin(2\alpha)-2\theta^2\alpha\right) \\
& -\frac{(1-\mu^2)f_2}{72I_Y E\bar{\theta}^4}\left[9\cos\theta(\sin(2\alpha)-2\alpha)-24\sin\alpha+8\sin^3\alpha+24\alpha\right] \\
& +\frac{(1-\mu^2)C_2 L}{8\beta\theta^3}(\alpha\sin(2\alpha)-\theta\sin(2\alpha)+2\theta\alpha+\cos(2\alpha)-1) \\
& +\frac{C_1 L}{24\beta\theta^3}\left(\begin{array}{l}3\theta\left[\left(2\alpha^2-\cos(2\alpha)+1\right)+\mu^2\left(2\alpha^2+\cos(2\alpha)-1\right)\right]+24\beta\alpha\theta^2 \\ -\left[\left(2\alpha^3-3\alpha\cos(2\alpha)-3\alpha+3\sin(2\alpha)\right)+\mu^2\left(2\alpha^3+3\alpha\cos(2\bar{\theta}z)+3\alpha-3\sin(2\alpha)\right)\right]\end{array}\right)
\end{aligned}
$$

$$
\begin{aligned}
u_y = {} & \frac{f_1}{96I_Y E\bar{\theta}^4}\left(\begin{array}{l}\mu^2\left\{2\alpha^4+3\left[-2\alpha^2\cos(2\alpha)+4\alpha\sin(2\alpha)+3\cos(2\alpha)-3\right]\right\} \\ +\left\{2\alpha^4-3\left[-2\alpha^2\cos(2\alpha)+4\alpha\sin(2\alpha)+3\cos(2\alpha)-3\right]\right\} \\ -6\theta^2\left[\mu^2\left(2\alpha^2-\cos(2\alpha)+1\right)+\left(2\alpha^2+\cos(2\alpha)-1\right)\right]-48\beta\theta^2\alpha^2\end{array}\right) \\
& +\frac{f_2}{72I_Y E\bar{\theta}^4}\left[\begin{array}{l}9\mu^2\cos\theta\left(2\alpha^2-\cos(2\alpha)+1\right)+9\cos\theta\left(2\alpha^2+\cos(2\alpha)-1\right) \\ +8\mu^2\left(6\cos\alpha+\cos^3\alpha-7\right)+8\left(3\cos\alpha-\cos^3\alpha-2\right)+72\beta\theta^2(\cos\alpha-1)\end{array}\right] \\
& +\frac{(1-\mu^2)C_1 L}{8\beta\theta^3}(\alpha\sin(2\alpha)-\theta\sin(2\alpha)+2\theta\alpha+\cos(2\alpha)-1) \\
& +\frac{C_2 L}{24\beta\theta^3}\left(\begin{array}{l}3\theta\left[\left(2\alpha^2+\cos(2\alpha)-1\right)+\mu^2\left(2\alpha^2-\cos(2\alpha)+1\right)\right]+24\beta\alpha\theta^2 \\ -\left[\left(2\alpha^3+3\alpha\cos(2\alpha)+3\alpha-3\sin(2\alpha)\right)+\mu^2\left(2\alpha^3-3\alpha\cos(2\alpha)-3\alpha+3\sin(2\alpha)\right)\right]\end{array}\right)
\end{aligned}
$$

LANZHOU UNIVERSITY

Mechanical model

The normal strain at position (x, y, z) is written as

$$\varepsilon_z = x\left(\begin{array}{l}\dfrac{(1-\mu^2)\sin(2\alpha)}{4I_Y E\bar{\theta}^2} f_1(\alpha^2-\theta^2)+\dfrac{(1-\mu^2)\sin(2\alpha)}{2I_Y E\bar{\theta}^2} f_2(\cos\theta-\cos\alpha) \\ +\dfrac{\left[\mu^2\sin^2\alpha+\cos^2\alpha\right]}{\beta\bar{\theta}L^2}C_1(\theta-\alpha)+\dfrac{(1-\mu^2)\sin(2\alpha)}{2\beta\bar{\theta}L^2}C_2(\theta-\alpha)\end{array}\right)$$

$$+y\left(\begin{array}{l}\dfrac{\mu^2\cos^2\alpha+\sin^2\alpha}{2I_Y E\bar{\theta}^2} f_1(\alpha^2-\theta^2)+\dfrac{\mu^2\cos^2\alpha+\sin^2\alpha}{I_Y E\bar{\theta}^2} f_2[\cos\theta-\cos\alpha] \\ +\dfrac{(1-\mu^2)\sin(2\alpha)}{2\beta\bar{\theta}L^2}C_1(\theta-\alpha)+\dfrac{\left[\mu^2\cos^2\alpha+\sin^2\alpha\right]}{\beta\bar{\theta}L^2}C_2(\theta-\alpha)\end{array}\right)$$

LANZHOU UNIVERSITY

Electromagnetic model

The electromagnetic model and the mechanical model are coupled by critical current density $J_c(\varepsilon_z)$.

$$E = E_c\left(\frac{J}{J_c(\varepsilon_z)}\right)^n \quad \Rightarrow \quad \sigma_s = \frac{J}{E} = \frac{J_c(\varepsilon_z)^n}{E_c} J^{1-n}$$

The critical current density $j_c(\varepsilon)$ for an axial strain is obtained from critical current data of axial strain tests,

$$J_c(\varepsilon_z) = J_{c0}(1 + a_1\varepsilon_z + a_2\varepsilon^2{}_z + a_3\varepsilon^3{}_z + a_4\varepsilon^4{}_z + a_5\varepsilon^5{}_z + a_6\varepsilon^6{}_z)$$

The governing equations describing the electromagnetic characteristics of the tape can be written as

$$\nabla \times \mathbf{E} = -\mu \frac{\partial \mathbf{H}}{\partial t} \qquad \nabla \times \mathbf{H} = \mathbf{J} \qquad \nabla \cdot \mathbf{H} = \mathbf{0} \qquad \mathbf{J} = \sigma_s \mathbf{E}$$

LANZHOU UNIVERSITY

Electromagnetic model

From the Ampere equations and the constitutive laws, one can derive the following **H**-formulation directly from the Faraday equation, leading to,

$$\mu\frac{\partial \mathbf{H}}{\partial t}+\nabla\times(\frac{1}{\sigma_s}\nabla\times\mathbf{H})=0$$

which is valid over the entire domain. To satisfy $\nabla\cdot\mathbf{H}=\mathbf{0}$,edge element is used.

The applied external fields are simulated by imposing a Dirichlet boundary condition on the air outer boundary

$$\left[H_{ext\text{-}x}\quad H_{ext-y}\quad H_{ext-z}\right]=\left[g_{ext\text{-}x}(t)\quad g_{ext\text{-}y}(t)\quad g_{ext\text{-}z}(t)\right]$$

The transport current I_t of tape is simulated by specifying a total transport current on the cross section S at the tape ends

$$I_0=\int_s \mathbf{J}\cdot\mathbf{n}dS$$

where **n** is the unit vector indicating the normal direction of the face S.

Contents

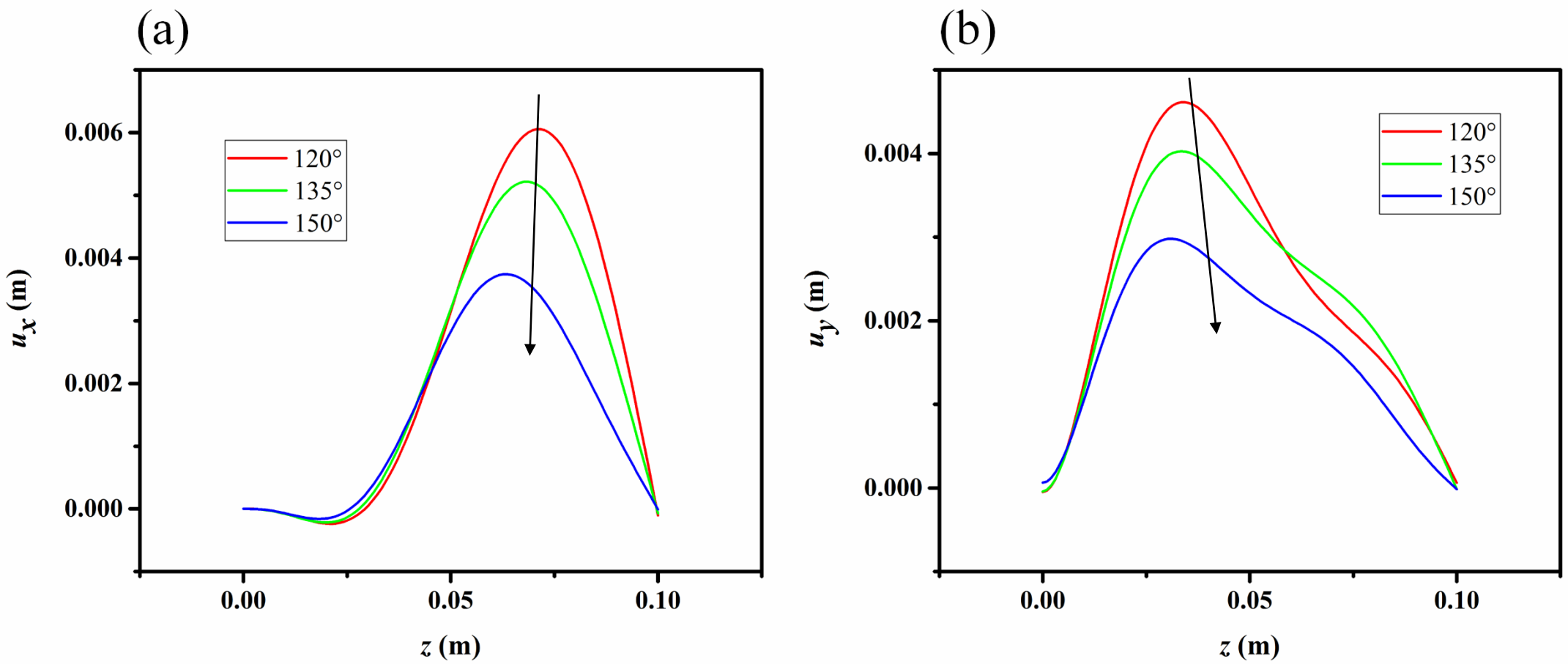

Variations of the deflections **(a)** u_x and (b) u_y of the tape with respect to the coordinate z.

- The deflection of the tape decreases as the twist angle increases under the same load.

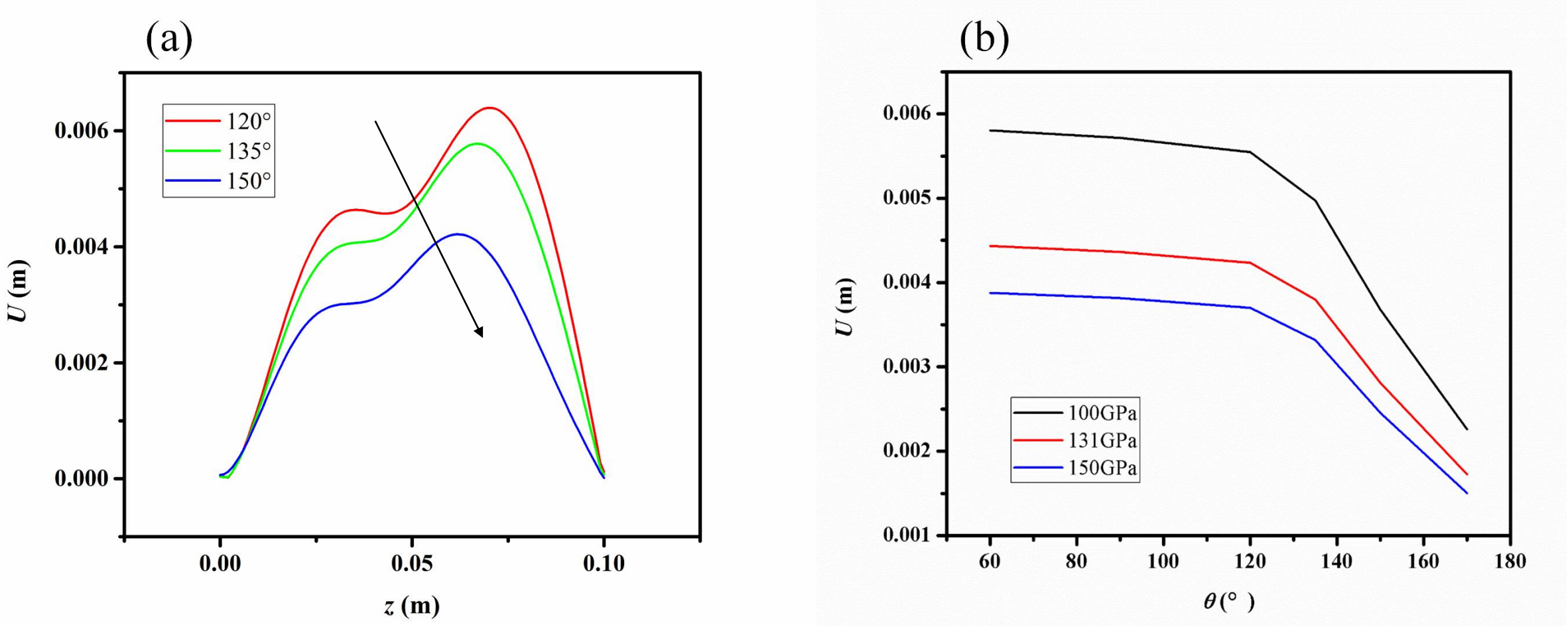

Variations of the total deflections U $(U=\sqrt{u_x^{\,2}+u_y^{\,2}})$ of the tape with respect to the coordinate z (a) and the twist angle θ (b).

- The total deflection decreases with the increase of the angle, and the increase of the twist angle increases the bending resistance of the tape.

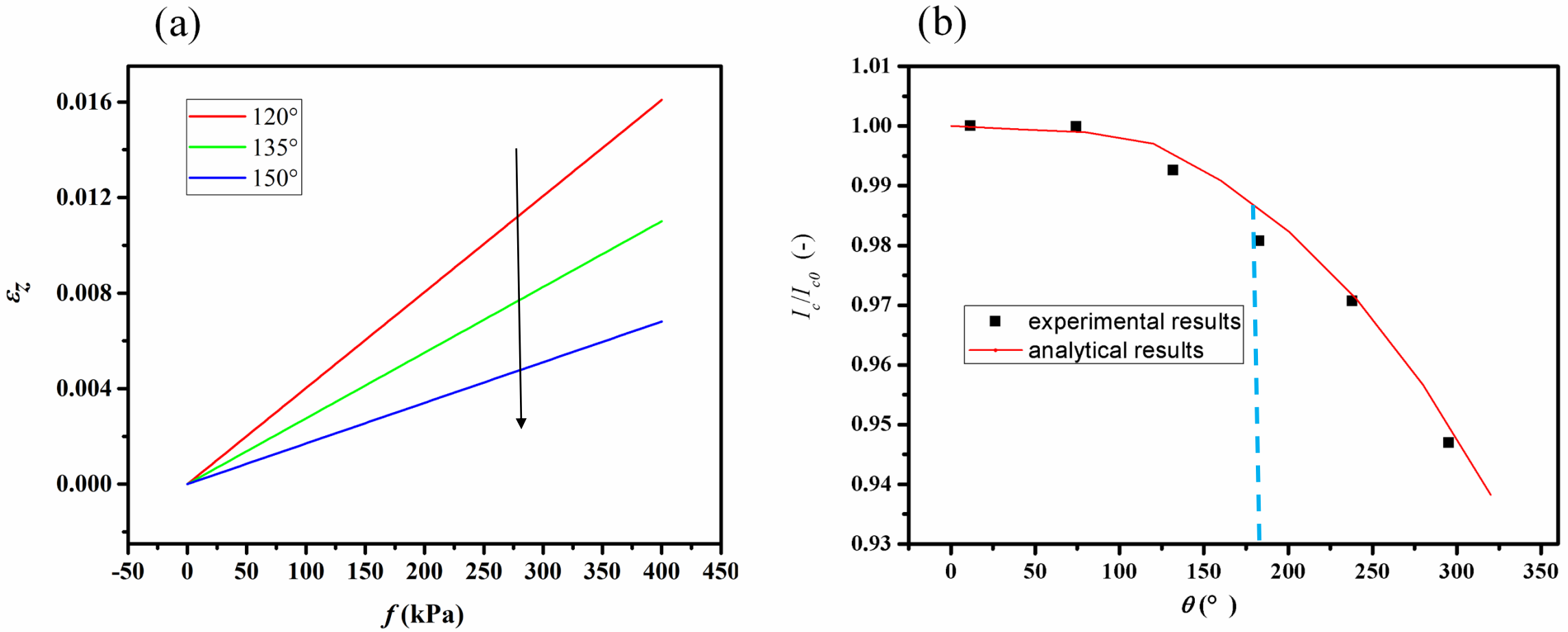

- The axial strain increases as the load increases. The strain decreases as the twist angle increases.
- The critical current decreases gradually with the increase of the angle, and the degradation occurs obviously after 180 degrees. Analytical and experimental results are in good agreement.

LANZHOU UNIVERSITY

Current density distribution

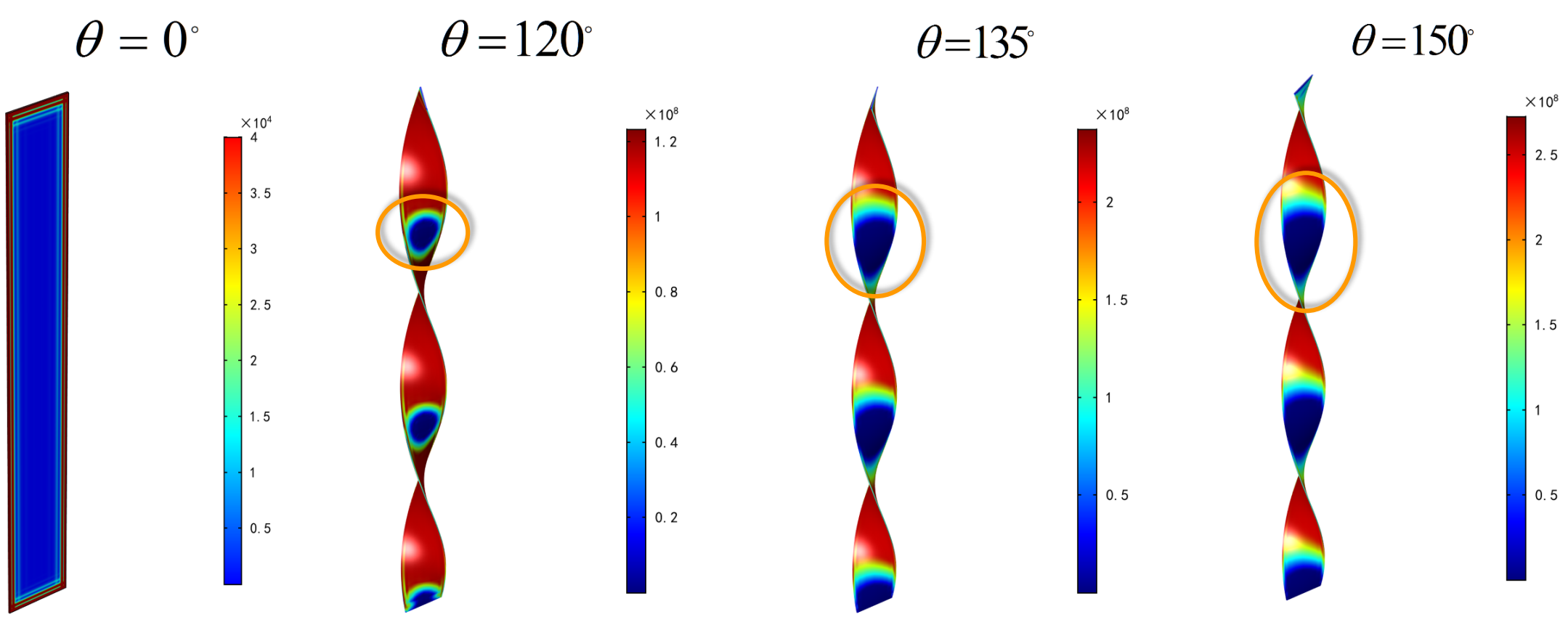

- The current is distributed over the edge of the superconducting tape when the tape is not twisted. The current is close to zero in the reverse position after twisting.
- The area where the current is zero increases as the twist angle increases.

LANZHOU UNIVERSITY

Effect of Load on Current Distribution

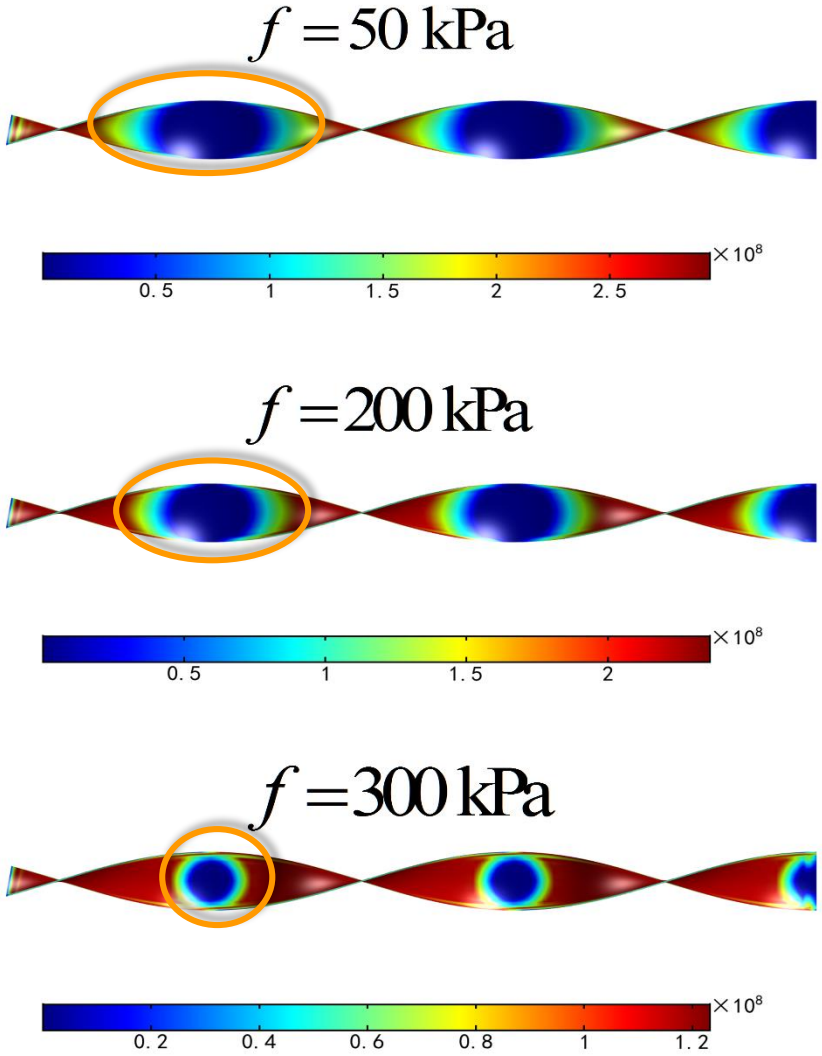

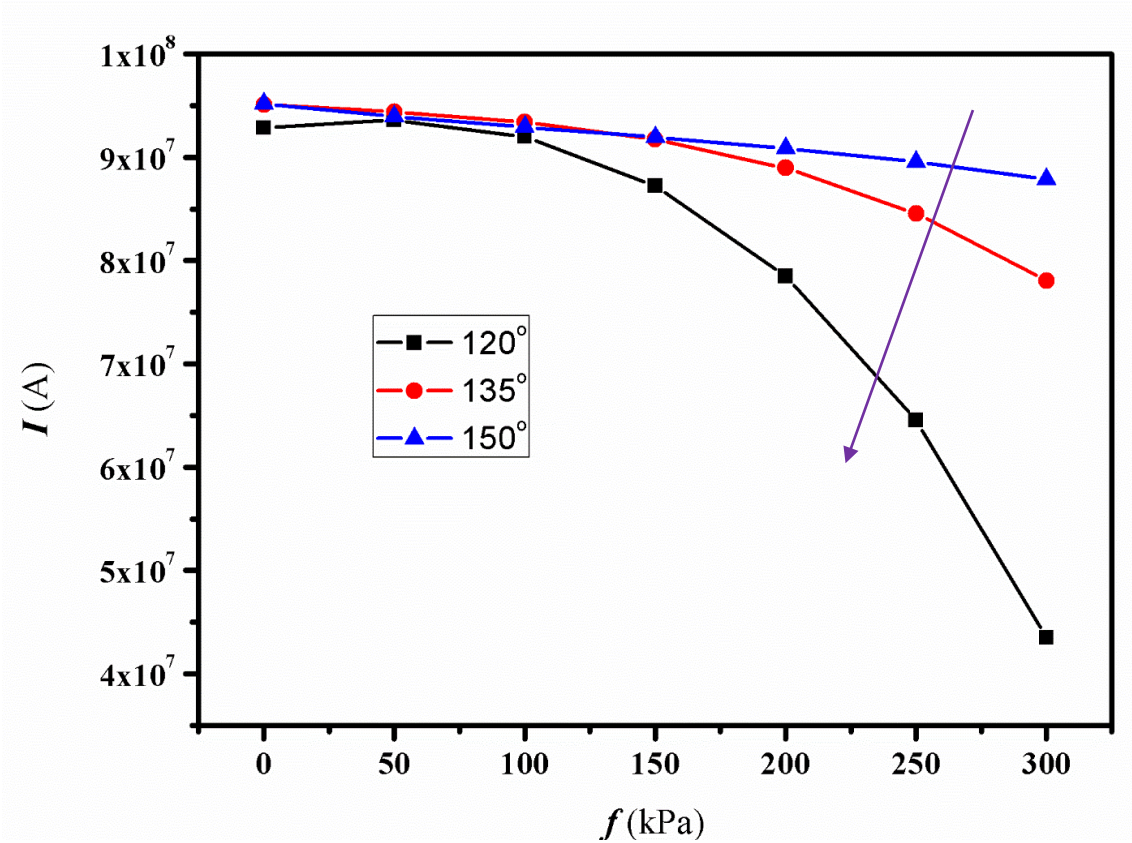

- As the load increases, the area of the current close to zero gradually decreases.
- The current decrease as the load increases.

LANZHOU UNIVERSITY

Effect of Load on AC Loss

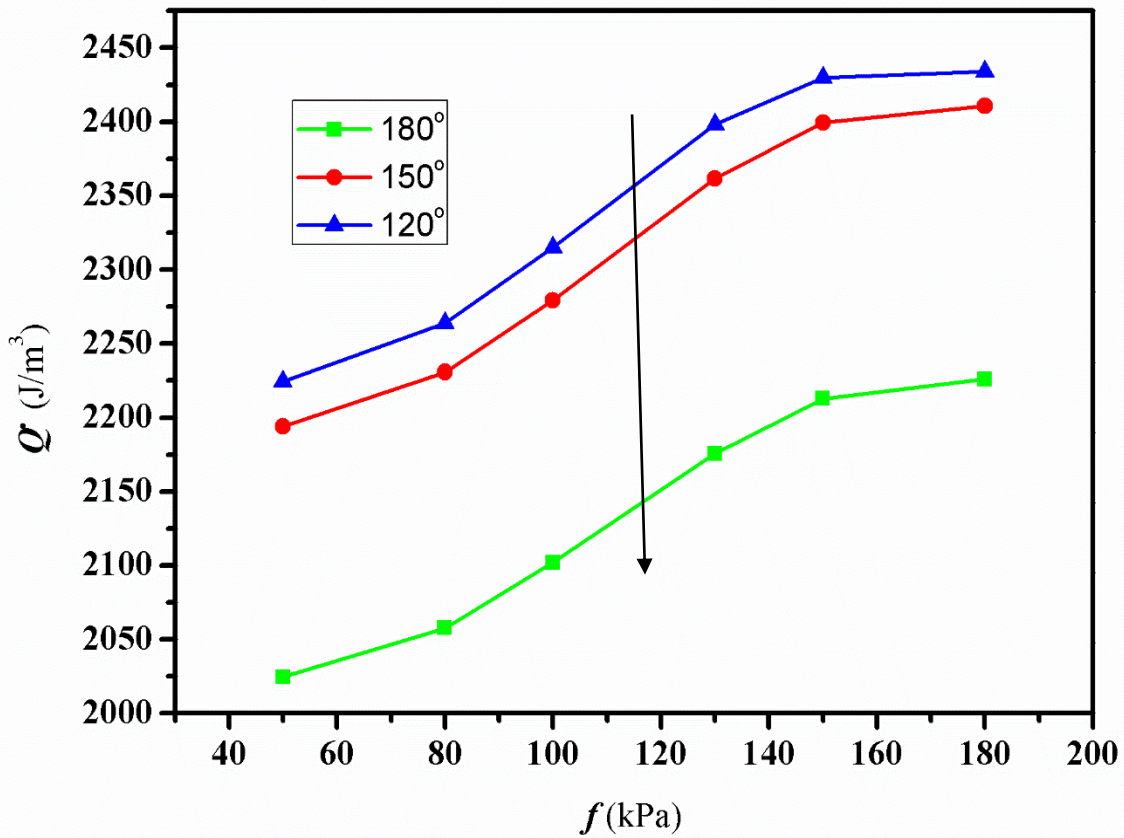

Effect of magnetic field on AC Loss

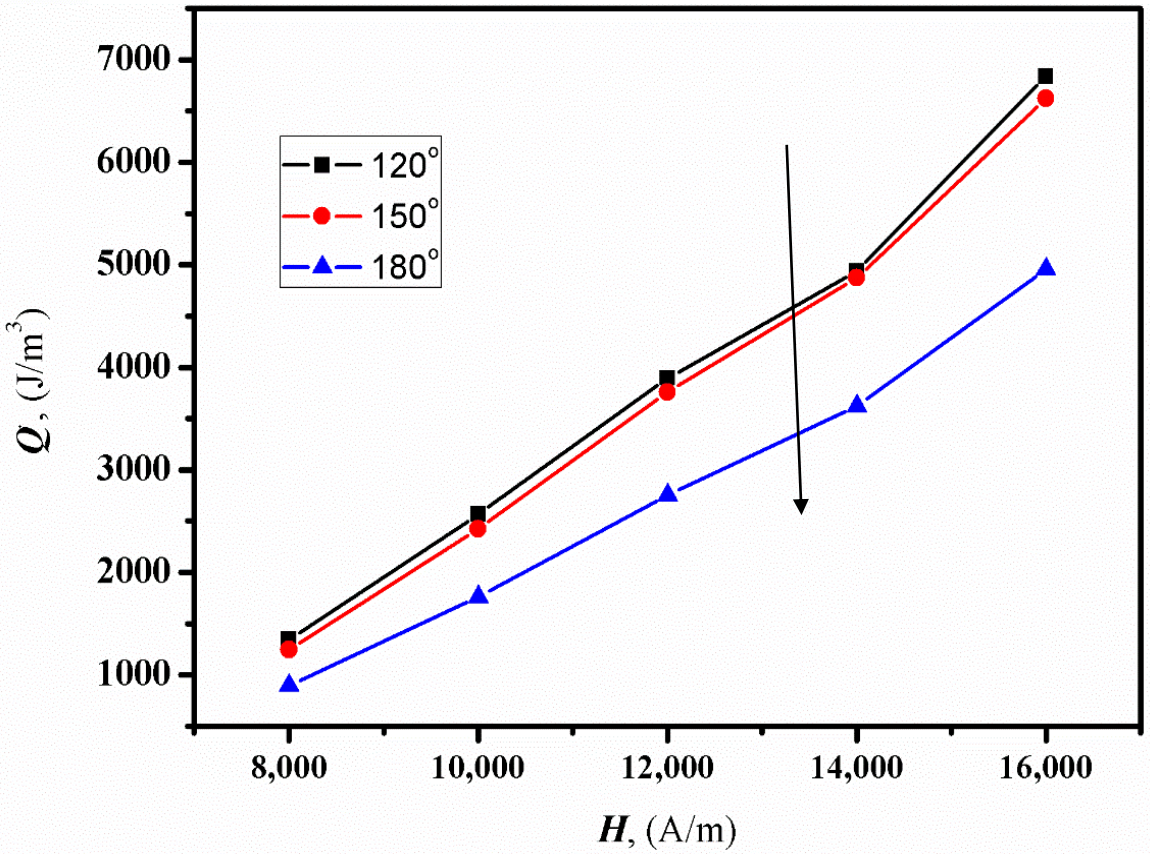

- The AC loss increases as the load and the magnetic field increase.
- The AC loss decreases as the twist angle increases, which means that the short twist pitch reduces the AC loss.

Contents

- A theoretical model for analyzing the mechanical and electrical properties of pre-twisted HTS tape was established.
- The twist angle has a significant effect on the mechanical properties of superconducting tapes. The deflection decreases with the increase of the twist angle, and the increase of the twist angle increases the bending resistance of the tape.
- The load and the twist angle have a significant effect on the transport performance and AC loss of the superconducting tape.
- It can be deduced that increasing the twist angle of the HTS tape (using the short pitch twist cable method) can enhance the mechanical properties and transport performance of the cable under the premise of ensuring that the superconducting tape is not damaged.

Thanks for your attention!